

Sinter forging of rapidly quenched eutectic $\text{Al}_2\text{O}_3\text{--ZrO}_2(\text{Y}_2\text{O}_3)$ -glass powders

Sreeram Balasubramanian, Hrishikesh Keshavan, W. Roger Cannon*

Ceramic and Materials Engineering, Rutgers University, 607 Taylor Road, Piscataway, NJ 08854, USA

Available online 19 February 2005

Abstract

Spray dried agglomerates of $\text{Al}_2\text{O}_3\text{--ZrO}_2$ (1% Y_2O_3) with 4 wt.% borosilicate glass were arc plasma sprayed and rapidly quenched into water. Because of the rapid quenching the particles $<25\ \mu\text{m}$ were mostly amorphous. After annealing 1 h at $1200\ ^\circ\text{C}$ the scale of the microstructure of the particles was on the order 30 nm. Hot forging of this powder yielded dense specimens with the width of the ZrO_2 phase still less than 100 nm. Since the particle size ranged from 5 to $25\ \mu\text{m}$ and the scale of the particle microstructure was $<100\ \text{nm}$, densification was controlled by creep of the particles rather than by the typical hot pressing mechanism of diffusion along the neck between particles to fill the pores. Thus, the scale of the microstructure controls densification rather than the particle size. These powders offer an alternate source for manufacturing nanostructured parts and should be more suitable for hot pressing or forging than nanoparticulate powders.

© 2005 Elsevier Ltd. All rights reserved.

Keywords: Nanocomposites; Hot pressing; Hot forging

1. Introduction

In the many studies currently underway on nanocrystalline ceramics, virtually all start with powders having particle sizes $<100\ \text{nm}$ diameter. The difficulty with this approach is that nanoparticulate powders are often costly, very difficult to process and have only occasionally resulted in dense ceramics with nanocrystalline grain size. Effective methods of inhibiting grain growth have not been developed. Specimens are also difficult to press or cast into a shape and densify into large parts. So far, in fact, to our knowledge no investigators have fabricated dense nanocrystalline ceramic specimens large enough to perform a statistical number of fracture tests.

Very stable two-phase microstructures in ceramics can be derived by cooling eutectic compositions from the melt. For instance, directionally solidified $\text{Al}_2\text{O}_3\text{--ZrO}_2$ lamellar structures are stable to coarsening and have excellent high temperature creep resistance.¹ The $\text{Al}_2\text{O}_3\text{--ZrO}_2$ eutectic is particularly interesting because of the well-developed lamellar structure, the limited solubility of Al_2O_3 and ZrO_2 in each other

and the high eutectic temperature. It is also well documented that the lamellar spacing is reduced as the solidification front velocity increases.² It is possible through rapid quenching, which produces a very rapid solidification front velocity, to achieve nanocrystalline lamellar spacing.³ In a previous paper plasma sprayed and water quenched particles cooled at the rate of about $10^4\ ^\circ\text{C/s}$, developed lamellar widths as small as 20 nm.⁴

Several attempts have been made to rapidly quench $\text{Al}_2\text{O}_3\text{--ZrO}_2$ powder, grind the powder and then consolidate it in order to make nanocrystalline monolithic parts.^{5–8} The advantage of using such a starting powder is that it already has a well mixed two phase microstructure extremely stable against coarsening. Thus, nanocrystalline ceramics might be sintered or hot pressed at moderate forming temperatures without appreciable growth in scale of the microstructure. Freim and McKittrick⁶ produced rapidly solidified eutectic $\text{Al}_2\text{O}_3\text{--ZrO}_2$ flakes ($50\text{--}100\ \mu\text{m}$ thick) with a microstructure of 40 nm thick lamellae. The flakes were milled to a $0.4\ \mu\text{m}$ particle size and sintered into $>99\%$ dense composites at 1500 and $1600\ ^\circ\text{C}$. At such high temperatures, however, the grain size coarsened to a few tenths of a micron. On the other hand, Bhaduri et al.⁷ who synthesized $\text{Al}_2\text{O}_3\text{--}10\%$

* Corresponding author. Tel.: +1 732 445 4718; fax: +1 732 445 8148.
E-mail address: cannon@alumina.rutgers.edu (W.R. Cannon).

ZrO₂ particles with a nanoscale microstructure by an auto ignition technique were able to maintain nanocrystalline microstructure by hot isostatic pressing compacts at 1200 °C. The as-quenched microstructure of this hypereutectic composition was not a lamellar structure but contained equiaxed ZrO₂ phases in an Al₂O₃ matrix. Claussen et al.⁵ rapidly quenched eutectic Al₂O₃–ZrO₂ powders from the melt. These coarse powders exhibited the lamellar structure but the results of the hot pressing study are not reported.

Two observations might be made. First, the lamellar structure is not ideal because it is too resistant to creep deformation¹ and second, efforts to grind the powder prior to hot pressing may not be necessary. Both of these suggestions are based on the contention that densification occurs by plastic deformation (creep) of the particles to fill the pores rather than by typical diffusional hot pressing mechanisms where pressure adds to the driving force and diffusion of matter along the intraparticle neck fills the pores. The mechanism of plastic flow by creep is sometime evoked during the early stages of hot pressing when stress concentrations at the contact point between particles is high.⁹ However, plastic deformation in ceramics increases rapidly as the scale of the microstructure gets finer and so if the scale of the microstructure of the powder is much smaller than the particle size, then plastic deformation should dominate. That is, the diffusional mode of densification by diffusion along the interparticle necks will be too slow and so plastic flow (creep) will dominate throughout the densification process rather than just in the early stages. The consequence is that the microstructure of the particles rather than the particle size will control the densification rate. In the current study the particles are spherical and coarse, which leads to ease in manufacturing but each particle has a nanoscale microstructure.

It may be further noted that superplastic deformation of particles might be expected because of their very fine microstructure.⁷ Most superplastic metals have two-phase microstructures to avoid grain growth. Recently, high strain rate superplasticity was reported by Kim et al.¹⁰ who used a tri-continuous microstructures of 30 vol.% alumina, 40 vol.% zirconia, 30 vol.% magnesium alumina spinel. Such microstructures are extremely difficult to fabricate by powder mixing since ultrafine powders mix poorly and are usually agglomerated. Well-dispersed two-phase microstructures are much more easily formed by rapid quenching of particles from the melt.

The composition chosen for this study was Al₂O₃–ZrO₂ eutectic + 1 mol% Y₂O₃ + 4% glass. Gust et al.¹¹ found that the creep rates of 3Y-TZP could be enhanced by a factor of about an order of magnitude by adding 1–5% of borosilicate silicate glass. In order to densify the composition in a reasonable time (<1 h) at low stresses (<200 MPa), 4 wt.% of a borosilicate glass was added to the powder. Attempts to densify the same composition without the glass yielded a factor of two slower densification rates. One percent Y₂O₃ rather than the usual 3% was used since less Y₂O₃ is needed to sta-

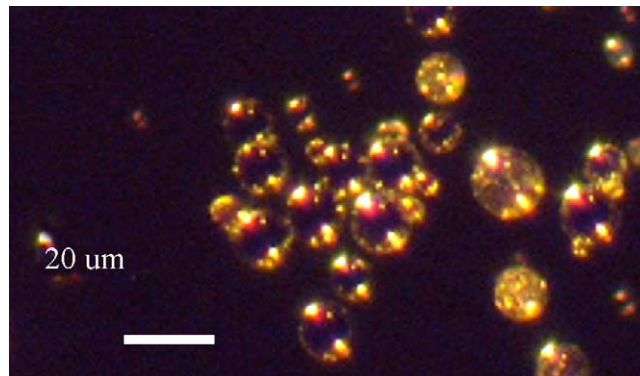


Fig. 1. Optical micrograph of particles plasma sprayed and quenched in water Al₂O₃–ZrO₂ (1% Y₂O₃) with 4% borosilicate glass. Most particles are fully transparent.

bilize ZrO₂ and leads to higher toughness values as noted by Bravo-Leon et al.¹²

2. Experimental

Powders were fabricated from commercial A16SG alumina (ALCOA), E-101 zirconia (Magnesium Electron Inc.) to form the approximate eutectic composition 42.2 wt.% ZrO₂ (1% Y₂O₃)–57.8 wt.% Al₂O₃ and then 4 wt.% borosilicate glass (5.8% Na₂O, 1.6% K₂O, 1.6% Al₂O₃, 16% B₂O₃, 75% SiO₂)^a was added. The powders were dispersed as an aqueous suspension (no binder was added) and then spray dried to obtain spherical particles. The Y₂O₃ and glass were attritor milled to submicrometer size prior to mixing. Spray dried agglomerates were heat treated to 1000 °C for 4 h to strengthen them before plasma spraying.

Spray dried agglomerates were arc plasma sprayed and rapidly quenched into water to attain the nanocrystalline microstructure. A radial powder injection, single electrode torch^b was used at 30 g/min spray rate in an argon and 10% hydrogen plasma. Power levels were 40 kW and a stand-off distance was 200 mm. The resulting powders were spherical and mostly transparent under an optical microscope as shown in Fig. 1. The transparency is a good indication that the particle microstructure was uniformly nanocrystalline since the scale of the microstructure is approximately a factor of 10 below the wavelength of light. Only a few percent of the powders under 38 μm diameter were not transparent, whereas about 25% of the particles over 38 μm were not transparent. The most common reason was lack of complete melting in the large particles.

Because the smaller particle size was more thoroughly melted and quenched, particles <25 μm was screened to use in the densification study. Powder compacts were placed in an alumina die for hot pressing. Throw-away dies for hot

^a Fusion Ceramics Inc., Carollton, OH composition, F-492.

^b Northwest Mettech Corp., Vancouver, Canada.

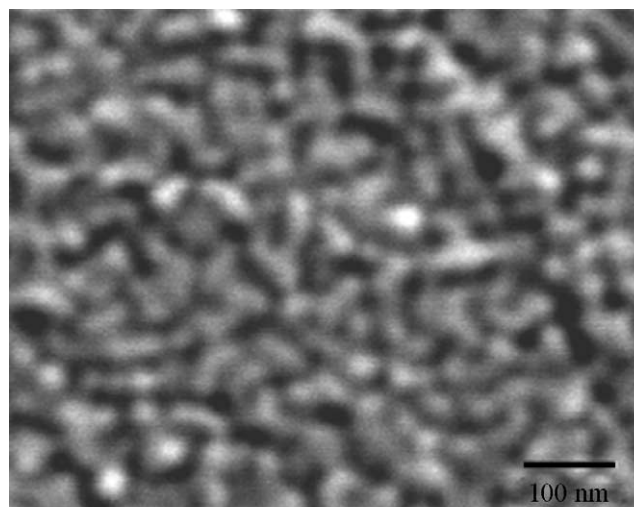
pressing were fabricated from commercial alumina tubes, 4.8 mm i.d., and alumina rods ground to fit. Specimens were hot pressed at 1250 °C for 0.5 h. The final hot pressing density was approximately 80% dense. Since higher densities are desired, the alumina die was then broken away and specimens were hot forged without constraint for an additional period of time at 1250 °C. Die wall friction and even sintering to the die wall reduced hot pressing effectiveness. Densification during sinter forging was more rapid because shear stresses are thought to aid in densification.

3. Results and discussion

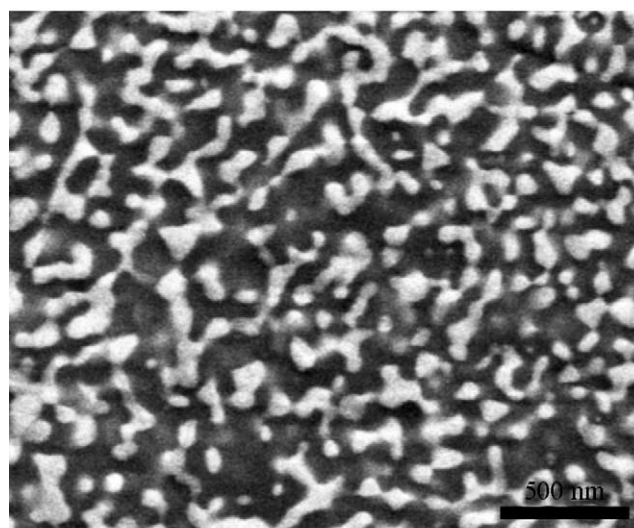
A high magnification scanning electron microscope (SEM) micrograph (in secondary electron mode) of cross-sections of an approximately 25 μm diameter particle plasma melted, quenched and annealed to 1200 °C for 1 h is shown in Fig. 2a. We were unable to image the microstructure of the as-quenched powder. The microstructure did not vary from the outer edge to the inside of the particle cross-section. The powder did not exhibit the typical lamellar eutectic microstructure observed by Zhou et al.⁴ for $\text{Al}_2\text{O}_3\text{--ZrO}_2$ but rather a cellular microstructure (or Chinese script). The scale of the microstructure, however, did not change appreciably. In a previous study by Zhou et al.,⁴ the mean lamellar width was 20 nm for a 20 μm diameter particle and 40 nm for a 100 μm particle. The size of the particle affects the quenching rate and, therefore, the scale of the microstructure. The quenching rate was calculated to be on the order of 10^4 °C/s and inversely related to the particle size.⁴ The phase width in Fig. 2a is about 30 nm for a 25 μm diameter particle and so the size scale is about the same as in the previous study.

Phase contrast under the SEM in Fig. 2 is due to atomic number contrast between ZrO_2 rich regions appearing brighter and Al_2O_3 rich regions appearing darker in these micrographs. In Fig. 2a there appears to be insufficient Al_2O_3 considering the eutectic composition is 67 vol.% Al_2O_3 and 33 vol.% ZrO_2 . Because of the rapid quenching rate a non-equilibrium amount of Al_2O_3 is in solid solution in the ZrO_2 which may lead to less contrast than is usually observed. Cosandey and co-workers¹³ found in a 20 wt.% Al_2O_3 in ZrO_2 material quenched from the plasma onto an iron substrate only 2.3% Al_2O_3 in solid solution in the ZrO_2 . According to equilibrium phase diagrams at the eutectic temperature 7% Al_2O_3 ¹⁴ is soluble in ZrO_2 but near room temperature >1% Al_2O_3 is soluble in ZrO_2 .¹⁵ X-ray spectra in Fig. 3 of the as-quenched powders indicate a mostly amorphous structure, but upon annealing to 1250 °C for 4 h the peaks sharpen. Grain growth, crystallization and dissolution of Al_2O_3 likely all contribute to peak sharpening of the tetragonal ZrO_2 peak. Particles remained transparent after annealing to 1200 °C indicating the phase growth was not excessive. After annealing at 1250 °C for greater than 8 h particles clouded very slightly.

The reason for adding glass to the eutectic composition was to enhance the creep rate.¹¹ Glass normally segregates



(a)



(b)

Fig. 2. High magnification SEM micrograph of (a) cross-section of particles plasma sprayed and quenched in water $\text{Al}_2\text{O}_3\text{--ZrO}_2$ (1% Y_2O_3) with 4% borosilicate glass annealed 1 h at 1200 °C, (b) High magnification micrograph of dense portion of sinter-forged specimen.

to grain boundaries and enhances grain boundary sliding or grain boundary diffusion, which leads to faster creep rates. TEM examination, which will be presented in a later paper, showed no evidence of a glassy grain boundary phase. It is more likely that the glass mixed thoroughly in the melt and formed zircon, ZrSiO_4 . In fact, there is some evidence of a developing zircon peak at $2\theta = 26.9$. Nevertheless hot pressing densification rates were a factor slower than when we did not add the glass. Other elements in the glass, i.e. Na_2O or K_2O may have also enhanced creep rates.

Fig. 4a and b show low magnification micrographs at two levels of densification, 80 and 95% dense. The arrows in Fig. 4a show three particles that have large pores in the center. Occasionally, spray dried powder agglomerates are hollow and the structure carries through to the plasma spraying

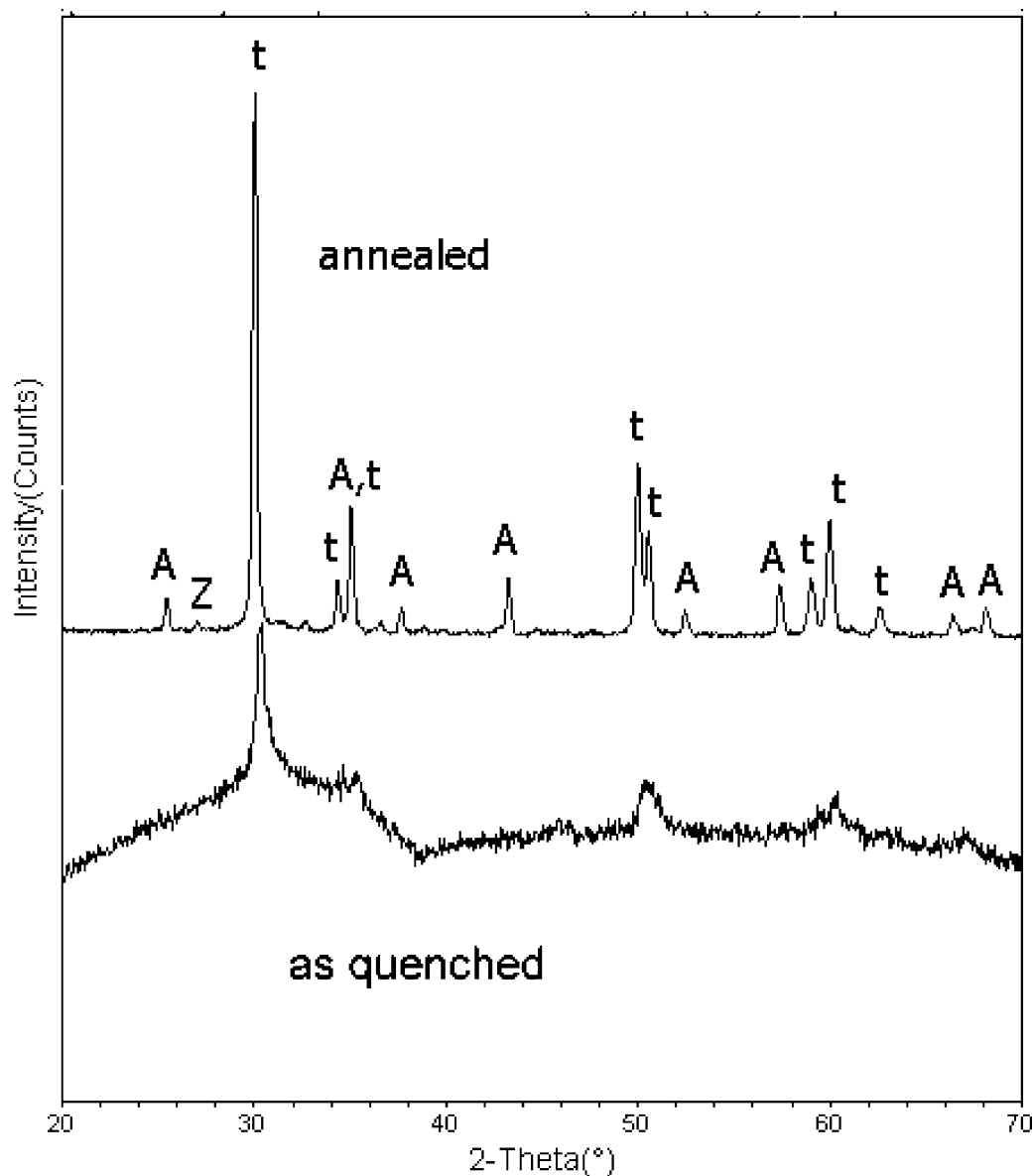


Fig. 3. X-ray pattern of powder, as-quenched and annealed at 1250 °C for 4 h. (A: α -alumina; t: tetragonal zirconia; Z: zircon).

process. Intraparticle pores can be avoided by either improved spray drying (for instance, higher solids in the feed suspensions) or plasma spraying the powder a second time. As densification proceeds, the few intraparticle pores also become smaller. The interparticle pores narrow and will eventually disappear. There are still remnants of interparticle pores in Fig. 4b. The highest densities were found near the center of the cylindrical forged specimens. Lower density porous regions were found near the outer edge of the specimen presumably because there was no radial constraint. Near the center micrographs indicated approximately 5% porosity.

Fig. 2b shows a high magnification view of a portion of the microstructure of the dense region of the specimen after forging. The scale of the features is approximately three times the initial size (Fig. 2a) and the development of elongated phases into more equiaxed phases. The approximate width of the zir-

conia phase is 80 nm. (measured by the planimetric method assuming elongated phases are strings of equiaxed particles). We also observed some regions of the microstructure near the contact points between particles that have quite different appearance, much less uniform. These will be discussed in a future paper. There is evidence for dynamic phase growth since after static annealing (under no load) at 1250 °C for 1 h the phase size was only 50 nm.

The fact that nearly full densification was accomplished within 23 min argues that the microstructure of the particles controlled the densification rate. The driving force for densification during hot forging is derived from the reduction in free surface (sintering) plus the applied stress. Since particles are on the order of 25 μm then the surface energy driving force is negligible in comparison to the pressure driving force. The diffusional densification strain rate during sinter forging is

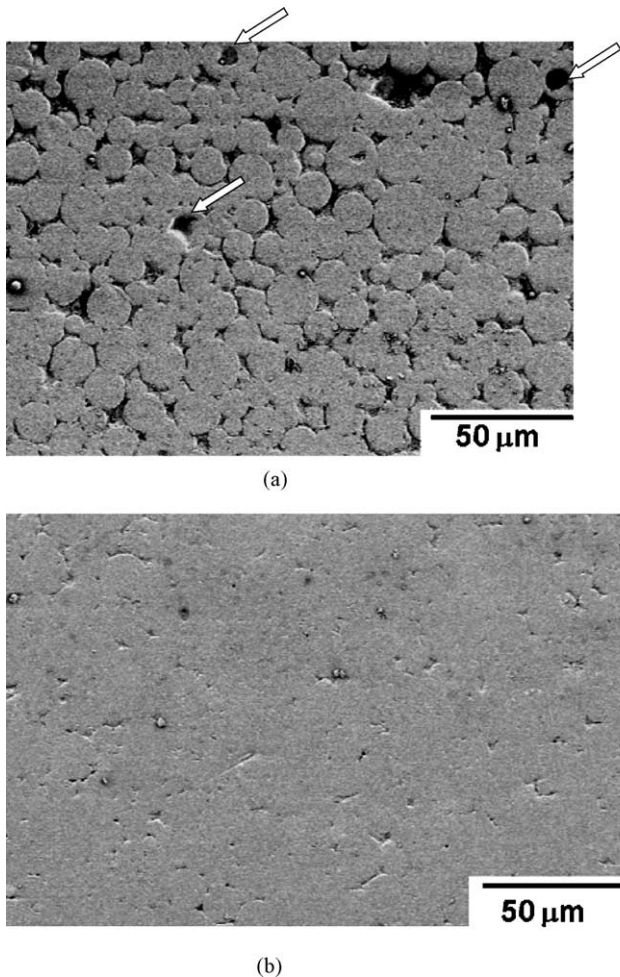


Fig. 4. SEM micrographs of sinter-forged $\text{Al}_2\text{O}_3\text{-ZrO}_2$ (1% Y_2O_3) with 4% borosilicate glass (a) 80% dense, hot pressed 30 min at 1250°C at 100 MPa (b) 95% dense 23 min at 1250°C constant load. Initial stress was 200 MPa.

then the product of a stress term and a kinetic. The kinetic term is a function of the diffusion coefficient and the diffusion distance. The kinetic term at a given temperature is about the same order of magnitude for densification and creep since they are both dependent on the diffusion distance. The creep strain rate is given by:

$$\dot{\epsilon} = \frac{A_c \sigma^n}{d^p}$$

where A/d^p is the kinetic term, d is the grain size, n is the grain size exponent, ~ 2 for superplastic creep and p the grain size exponent typically 2 or 3. The forging rate in this study was on the order of 10^{-3} s^{-1} in the early stages to 10^{-4} s^{-1} in the latter stages. Wakai et al.¹⁷ measured the creep rate of 60 vol.% $\text{Al}_2\text{O}_3\text{-40 vol.}\%$ ZrO_2 (3 Y_2O_3) to be $2 \times 10^{-7} \text{ s}^{-1}$ at 50 MPa and 1250°C . Correcting for stress using $n=2$, yields a creep rate of 3.2×10^{-6} at 200 MPa. In their study the Al_2O_3 grain size was $1 \mu\text{m}$ and the ZrO_2 grain size $0.6 \mu\text{m}$. If densification were based on the $25 \mu\text{m}$ particle, $d=25 \mu\text{m}$. For $p=2$ the corrected rate would be $\sim 5 \times 10^{-9}$. Thus, den-

sification rates are 6 orders of magnitude faster than the corrected rate for a $25 \mu\text{m}$ -sized particle. Thus, it is clear that the microstructure of the particle controls the densification rate.

The advantage of using powders of spherical particles in the size range of $5\text{--}25 \mu\text{m}$ is obvious. Die filling during manufacturing is greatly improved even over conventional micron sized powders but is enormously improved over nanocrystalline powder. Furthermore, gas adsorption on these low specific surface area powders is minimal and out-gassing is rapid. Plasma spraying/quenching of commercial powder will also add little to the cost of powder production. Thus, these powders would seem to have considerable advantage for hot pressing. There are, however, some restrictions on the materials that can be used in this way as a source for hot pressing. Although only oxides can be plasma spray easily, some non-oxide powders have also been plasma sprayed. Furthermore, to inhibit grain growth two or more phases are advantageous and so compositions must be chosen from phase diagrams containing multiple phases.

4. Conclusion

$\text{Al}_2\text{O}_3\text{-ZrO}_2$ containing glass were hot forged to nearly full density while retaining the nanocrystalline microstructure. The grain size was apparently sufficiently small that the rate of deformation of the particles by creep was sufficient to densify the specimens under hot forging conditions in a short period in time.

Acknowledgements

This work was supported by Department of Energy, Basic Energy Sciences. We wish to acknowledge Evgenia Pekarskaya for Fig. 2b and for helpful suggestions.

References

1. Sayir, A. and Farmer, S. C., The effect of the microstructure on mechanical properties of directionally solidified $\text{Al}_2\text{O}_3/\text{ZrO}_2$ (2 Y_2O_3) eutectic. *Acta Mater.*, 2000, **48**, 4691.
2. Bourban, S., Karapatis, N., Hofmann, H. and Kurz, W., Solidification microstructure of laser remelted $\text{Al}_2\text{O}_3\text{-ZrO}_2$ eutectic. *Acta Mater.*, 1997, **45**, 5069.
3. Calderon-Moreno, J. M. and Yoshimura, M., Nanocomposites from melt in the system $\text{Al}_2\text{O}_3\text{-YAG-ZrO}_2$. *Scripta Mater.*, 2001, **44**, 2153.
4. Zhou, X., Shukla, V., Cannon, W. R. and Kear, B. H., Metastable phase formation in plasma sprayed zirconia (yttria)-alumina powders. *J. Am. Ceram. Soc.*, 2 A.D., **86**, 1415.
5. Claussen, N., Lindemann, G. and Petzow, G., Rapid solidification in the $\text{Al}_2\text{O}_3\text{-ZrO}_2$ system. *Ceram. Int.*, 1983, **9**, 83.
6. Freim, J. and McKittrick, J., Modeling and fabrication of fine-grain alumina-zirconia composites produced from nanocrystalline precursors. *J. Am. Ceram. Soc.*, 1998, **81**, 1773.

7. Bhaduri, S., Bhaduri, S. B. and Zhou, E., Auto ignition synthesis and consolidation of $\text{Al}_2\text{O}_3\text{-ZrO}_2$ nano/nano composite powders. *J. Mater. Res.*, 1998, **13**, 156.
8. Bhaduri, S. and Bhaduri, S. B., Microstructural and mechanical properties of nanocrystalline spinel and related composites. *Ceram. Int.*, 2002, **28**, 153.
9. Coble, R., Diffusion models for hot pressing with surface energy and pressure effects as driving forces. *J. Appl. Phys.*, 1970, **41**, 4798.
10. Kim, B. N., Hiraga, K., Morita, K. and Sakka, Y., A high-strain-rate superplastic ceramic. *Nature*, 2001, **413**, 288.
11. Gust, M., Goo, G., Wolfenstine, J. and Mecartney, M. L., Influence of amorphous grain boundary phases on the superplastic behavior of 3-mole%-yttria-stabilized superplastic. *J. Am. Ceram. Soc.*, 1993, **76**, 1681.
12. Bravo-Leon, A., Morikawa, Y., Kawahara, M. and Mayo, M. J., Fracture toughness of nanocrystalline tetragonal zirconia with low yttria content. *Acta Mater.*, 2002, **50**, 4555.
13. Lui, F., Cosandey, F., Zhou, X. and Kear, B. H., Nanophase decomposition in plasma sprayed $\text{ZrO}_2(\text{Y}_2\text{O}_3)/\text{Al}_2\text{O}_3$ coatings. *Ceram. Trans.*, 2004, **148**, 91–100.
14. Alper, A. M., McNally, R. N. and Doman, R. C., Phase equilibria in the $\text{Al}_2\text{O}_3\text{-ZrO}_2$ system. *J. Am. Ceram. Soc.*, 1964, **43**, 642.
15. Levin, E. M. and McMurdie, H. F., $\text{Al}_2\text{O}_3\text{-ZrO}_2$ phase diagram. 1975 [Fig. 4378].
17. Wakai, F., Kodama, Y., Sakaguchi, S., Murayama, N., Kato, H. and Nagano, T., *Superplastic Deformation of $\text{Al}_2\text{O}_3/\text{ZrO}_2$ Duplex Composites*, vol.7, ed. M. Doyama, S. Somiya and Robert P. H. Chang. MRS, Tokyo, Japan, 1989, pp. 259–266.